VACUUM

ScienceDirect

Vacuum

Supports *open access*

4.2
CiteScore

2.906
Impact Factor

Articles & Issues About Publish Search in this jou Submit your article Guide for authors

About the journal

Aims and scope | Editorial board | Abstracting and indexing

Editor-in-Chief

L.G. Hultman
Linköping University, Linköping, Sweden

Editor

P. Eklund
Linköping University, Linköping, Sweden

Associate Editors

O.B. Malyshev
Sci-Tech Daresbury, Warrington, Cheshire, United Kingdom

P. Mayrhofer
TU Wien University, Wien, Austria

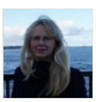

ISSN: 0042-207X

Vacuum

Supports *open access*

Volume 182

December 2020

Research article ○ Abstract only
Numerical simulation of neoclassical tearing modes induced by resonant magnetic perturbations in tokamak plasmas
Shuang-Shuang Lu, Yue Liu, Lai Wei
Article 109656

Purchase PDF Article preview

Research article ○ Abstract only
Observation of the development of pulsed discharge inside a bubble under water using ICCD cameras
Katsuyuki Takahashi, Hirotoshi Takayama, Shota Kobayashi, Masahiro Takeda, ... Takao Namihira
Article 109690

Purchase PDF Article preview

Research article ○ Abstract only
Nitrogen ion beam thinning of a-SiCN diaphragm for environmental cell prepared by low-energy ion beam enhanced chemical vapor deposition
Takaomi Matsutani, Yuki Tai, Tadahiro Kawasaki
Article 109770

Purchase PDF Article preview

Special Section on the Creation, Control and Investigation of Defects in d^0 Ferromagnetic Materials (d^0 Ferromagnetic Materials); Edited by Jitendra Pal Singh, Keun Hwa Chae and Sangsul Lee

---

Research article ○ Abstract only
Emergence of magnetic behavior in AB-stacked bilayer graphene via Fe-doping
Renu Singla, Jyoti Thakur, Priti Rani, Sarvesh Kumar, ... Manish K. Kashyap
Article 109685

Purchase PDF Article preview

Research article ○ Abstract only
Electronic, magnetic and optical properties of monolayer (ML) hexagonal ZnSe on vacancy defects at Zn sites from DFT-1/2 approach
D.P. Rai, Amel Laref, M. Khuili, Samah Al-Qaisi, ... Dat D. Vo
Article 109597

Purchase PDF Article preview

Research article ○ Abstract only
d^0 Ferromagnetism in Ag-doped monoclinic ZrO_2 compounds
L. Chouhan, G. Bouzerar, S.K. Srivastava
Article 109716

Purchase PDF Article preview

Research article ○ Abstract only
Epitaxial 4H–SiC based Schottky diode temperature sensors in ultra-low current range
Vibhor Kumar, Jyoti Verma, A.S. Maan, Jamil Akhtar
Article 109590

Purchase PDF Article preview

Research article ○ Abstract only

Structural, functional and magnetic ordering modifications in graphene oxide and graphite by 100 MeV gold ion irradiation

Pankaj Singh Rawat, R.C. Srivastava, Gagan Dixit, K. Asokan

Article 109700

Purchase PDF Article preview

Research article ○ Abstract only

Exploration of structural, morphological and magnetic properties of transition metal doped SnO_2 films grown using pulsed laser deposition

Shalendra Kumar

Article 109725

Purchase PDF Article preview

Research article ○ Abstract only

Induction of half-metallic ferromagnetism in BaS semiconductor via Cr-doping

Poonam Mehra, Hardev S. Saini, Satyender Sinhmar, Jyoti Thakur, Manish K. Kashyap

Article 109760

Purchase PDF Article preview

Short Communication Papers

Short communication *Open access*

Smart gas dosage by a peristaltic pump for reactive RF sputtering of composition spread combinatorial hafnium-oxy-nitride layers

György Sáfrán, Noémi Szász, Gergely Dobrik, Benjámin Kalas, Miklós Serényi

Article 109675

Download PDF Article preview

Short communication ○ Abstract only

Formation of irregular morphology on nanostructured surface by gas cluster ion beam

Vasiliy Pelenovich, Xiaomei Zeng, Wenbin Zuo, Alexander Tolstogouzov, ... Bing Yang

Article 109705

Purchase PDF Article preview

Short communication ○ Abstract only

Pre-hole Friction Stir Spot Welding (PFSSW) for dissimilar welding of AA2219 to AA3003 sheets

Yang Gao, Yuan Liang, Xiaoqiang Ren, Moslem Paidar

Article 109688

Purchase PDF Article preview

Short communication ○ Abstract only

Low-temperature growth of high-quality *a*-plane GaN epitaxial films on lattice-matched $LaAlO_3$ substrates

Jinghan Liang, Yuhui Yang, Deqi Kong, Zhibang Song, ... Guoqiang Li

Article 109687

Purchase PDF Article preview

Short communication ○ Abstract only

Improving the morphological, optical, and photocatalytic properties of octahedral Zn_2SnO_4 using *Garcinia mangostana* fruit peel extract

Eka Angasa, Yulia Eka Putri, Zulhadjri, Novesar Jamarun, Syukri Arief

Article 109719

Purchase PDF Article preview

Short communication ○ Abstract only

Experiment and simulation on the high-speed milling mechanism of aluminum alloy 7050-T7451

Zhang Ping, Xiujie Yue, Han Shuangfeng, Song Ailing, ... Yu Xiao

Article 109778

Purchase PDF Article preview

Short communication ○ Abstract only

Enhancing anti-wear and anti-corrosion performance of cold spraying aluminum coating by high current pulsed electron beam irradiation

Feng Guo, Wei Jiang, Guangze Tang, Zhiwen Xie, ... Lijun Liu

Article 109772

Purchase PDF Article preview

Short communication ○ Abstract only

Single-crystal growth of n-type $SnS_{0.95}$ by the temperature-gradient technique

Yinong Yin, Jianfeng Cai, Hongxiang Wang, Yukun Xiao, ... Jun Jiang

Article 109789

Purchase PDF Article preview

Short communication ○ Abstract only

Atomistic strain and structural analysis of 120 MeV Ni ions irradiated CdSe nanocrystals through molecular dynamics simulation method

Debojyoti Nath, Fouran Singh, Ratan Das

Article 109794

Purchase PDF Article preview

Regular Articles

Research article ○ Abstract only

Hydrogen adsorption on $L1_2$-Al_3X(X = Zr, Sc) surface and its diffusion in the bulk: A first-principles study

Yu Liu, XieYi Zhang, Zheng-Bing Xiao, YuanChun Huang

Article 109680

Purchase PDF Article preview

Research article ○ Abstract only

Effects of triaxial strain on carrier activity, carrier lifetime, and absorption spectrum of (S, Se, Te) and 2 N Co-doped ZnO

Qingyu Hou, Shulin Sha

Article 109684

Purchase PDF Article preview

Research article ○ Abstract only

Investigation on structural stability of as-cast $Al_{0.5}CrCuFeMnTi$ high entropy alloy

Zhi-Sheng Nong, Hao-Yu Wang, Da-Peng Wang, Jing-Chuan Zhu

Article 109686

Purchase PDF Article preview

Research article ○ Abstract only

Investigation on the influence of the gas flow mode around substrate on the deposition of diamond films in an overmoded MPCVD reactor chamber

B. Wang, J. Weng, Z.T. Wang, J.H. Wang, ... L.W. Xiong

Article 109659

Purchase PDF Article preview

Research article ○ Abstract only

Effect of sequential isochronal annealing on the structure and migration behaviour of selenium-ion implanted in glassy carbon

S.A. Adeojo, J.B. Malherbe, E.G. Njoroge, M. Mlambo, ... T.T. Hlatshwayo

Article 109689

Purchase PDF Article preview

Research article ○ Abstract only

Designed synthesis of 2D multilayer $CuCo_2S_4$ nanomaterials for high-performance asymmetric supercapacitors

Jibo Jiang, Yukai Chen, Xiaomin Hu, Haishan Cong, ... Sheng Han

Article 109698

Purchase PDF Article preview

Research article ○ Abstract only

Hollow SnO_2/Zn_2SnO_4 cubes with porous shells towards n-butylamine sensing and photocatalytic applications

Zhengdao Li, Yanli Zhao, Liuqing Hua, Dongqin Bi, ... Yong Zhou

Article 109693

Purchase PDF Article preview

Research article ○ Abstract only

Ti^{3+} and oxygen defects controlled colored TiO_2 nanoparticles by continuous spray pyrolysis

Charu Dwivedi, Tauheed Mohammad, Vinod Kumar, Viresh Dutta

Article 109612

Purchase PDF Article preview

Research article ○ Abstract only

Scanning electron imaging with vertically aligned carbon nanotube (CNT) based cold cathode electron beam (C-beam)

Ha Rim Lee, Da Woon Kim, Ok Jung Hwang, Boklae Cho, Kyu Chang Park

Article 109696

Purchase PDF Article preview

Research article ○ Abstract only

Resolving transient discharge cycle behaviour in modulated inductive plasmas

R. Georg, A.R. Chadwick, B.B. Dally, G. Herdrich

Article 109636

Purchase PDF Article preview

Research article ○ Abstract only

Chemisorbed CO_2 molecules on ZnO nanowires (100 nm) surface leading towards enhanced piezoelectric voltage

Mansoor Ahmad, M.K. Ahmad, N. Nafarizal, C.F. Soon, ... M.H. Mamat

Article 109565

Purchase PDF Article preview

Research article ○ Abstract only

Enhancement in light-emission efficiency of InGaN/GaN multiple quantum well layer by a porous-GaN mirror

Chongchong Zhao, Xiaokun Yang, Bin Wei, Jie Liu, ... Hongdi Xiao

Article 109669

Purchase PDF Article preview

Research article ○ Abstract only

A promising post-additive manufacturing surface modification for tailoring gradient nanostructure and harmonic structure in Co–Cr–Mo alloy

Auezhan Amanov

Article 109702

Purchase PDF Article preview

Research article ○ Abstract only

Alternative anode geometry for magnetron sputtering

Kleber Alexandre Petroski, Julio César Sagás

Article 109703

Purchase PDF Article preview

Research article ○ Abstract only

Enhanced red shift in optical absorption edge and photoelectrochemical performance of N-incorporated gallium oxide nanostructures

P.R. Jubu, F.K. Yam, Khaled M. Chahrour

Article 109704

Purchase PDF Article preview

Research article ○ Abstract only

Synthesis and characterizations of $Pd/Mn(Mn_{1.36}Pd_{0.64})O_4$ nanocomposite: An experimental and theoretical approach

Ramesh Sivasamy, Potu Venugopal, Karrothu Varun Kumar, Rodrigo Espinoza-González

Article 109683

Purchase PDF Article preview

Research article ○ Abstract only

Effect of vacuum level on the interfacial reactions between K417 superalloy and Y_2O_3 crucibles

Jinpeng Li, Huarui Zhang, Ming Gao, Qingling Li, ... Hu Zhang

Article 109701

Purchase PDF Article preview

Research article ○ Abstract only

The role of microstructure on corrosion fatigue behavior of thick-plate Ti–6Al–4V joint via vacuum electron beam welding
C.Y. Zeng, Y.P. Zhang, J.L. Hu, B. Hou, ... Y. Zhou
Article 109714

Purchase PDF Article preview

Research article ○ Abstract only
Growth of hydrophilic graphene oxide layers using continuous laser ablation
Vishakha Kaushik, Sachin Pathak, H. Sharma, A.K. Shukla, V.D. Vankar
Article 109721

Purchase PDF Article preview

Research article ○ Abstract only
Seed-induced $NiCo_2S_4$ nanosheets with integral ultrafine nanocrystals for efficient supercapacitors
Hao Zheng, Huiling Zhu, Meng Zhang, Mengmeng Zhang, ... Hongzhi Cui
Article 109618

Purchase PDF Article preview

Research article ○ Abstract only
Investigation of the electronic and magnetic properties of low-dimensional $FeCl_2$ derivatives by first-principles calculations
Yuyuan Zhu, Huili Li, Tong Chen, Desheng Liu, QingHua Zhou
Article 109694

Purchase PDF Article preview

Research article ○ Abstract only
Catalytic oxidation/photocatalytic degradation of ethyl mercaptan on α-MnO_2@$H_4Nb_6O_{17}$-NS nanocomposite
Chunli Guo, Jichao Zhu, Jie He, Lifang Hu, ... Dewei Li
Article 109718

Purchase PDF Article preview

Research article ○ Abstract only
Thin film LiV_3O_8 nanorod formation through Pulsed Laser Deposition and the effect of heat treatment
Rojin Varghese, V. Shobin Vijay, S. Rajesh, A. Sakunthala, ... Raman Sankar
Article 109722

Purchase PDF Article preview

Research article ○ Abstract only
Evolution of aging precipitates in an Al–Li alloy with 1.5 wt% Li concentration
Hong Ning, Jin-feng Li, Peng-cheng Ma, Yong-lai Chen, ... Rui-feng Zhang
Article 109677

Purchase PDF Article preview

Research article ○ Abstract only
Characterization of sequential physical vapor deposited methylammonium lead tri-iodide perovskite thin films
J.N. Fru, N. Nombona, M. Diale
Article 109727

Purchase PDF Article preview

Research article ○ Abstract only

Metal-organic framework derived α-Fe_2O_3 nano-octahedron with oxygen vacancies for realizing outstanding energy storage performance

Shanshan Xiong, XianMeng Lin, Shuai Liu, Shuting Weng, ... Jianrong Cheng

Article 109692

Purchase PDF Article preview

Research article ○ Abstract only

Magnetic and optical properties of (Mn, Co) co-doped SnO_2

Long Lin, Ruixin Chen, Chaozheng He, Hualong Tao, ... Jisheng Zhang

Article 109681

Purchase PDF Article preview

Research article ○ Abstract only

Optical actinometric measurements of nitrogen impurity in Ar/He microwave discharge during wall cleaning of MT-I spherical tokamak

Farah Deeba, A. Qayyum, M.U. Naseer, S. Hussain

Article 109672

Purchase PDF Article preview

Research article ○ Abstract only

Pulse ion annealing of silicon layers with silver nanoparticles formed by ion implantation

A.L. Stepanov, R.I. Batalov, R.M. Bayazitov, A.M. Rogov

Article 109724

Purchase PDF Article preview

Research article ○ Abstract only

Two unexplored two-dimensional MSe_2 (M = Cd, Zn) structures as the photocatalysts of water splitting and the enhancement of their performances by strain

Xinyi Yang, Yungang Zhou, Junjie He

Article 109728

Purchase PDF Article preview

Research article ○ Abstract only

Solubility limit of nitrogen in Fe–Cr–C–N alloy melt under reduced N_2 partial pressure

Min-Kyu Paek, Daniel Lindberg, Jong-Jin Pak

Article 109726

Purchase PDF Article preview

Research article ○ Abstract only

Underlying reasons of poor mechanical performance of thick plate aluminum-copper alloy vacuum electron beam welded joints

Guoqing Chen, Junpeng Liu, Zhibo Dong, Xi Shu, Binggang Zhang

Article 109667

Purchase PDF Article preview

Research article ○ Abstract only

Exploring cavitation erosion resistance of ZrN nanocrystalline coating prepared by double-cathode glow discharge plasma

Research article ○ Abstract only

Effect of heat input on microstructure and mechanical properties of IC10 Ni_3Al-based superalloy electron beam welding joint

Wenjun Sun, Shanlin Wang, Min Hong, Jijun Xin, ... Yuhua Chen

Article 109765

Purchase PDF Article preview

Research article ○ Abstract only

Experimental tests of the vacuum sealing performance of the ConFlat flange 25 for the HL-2M divertor pipeline circuit

Long Zhang, Yong Lu, Lijun Cai, Yunfeng Li, ... Yinglong Yuan

Article 109747

Purchase PDF Article preview

Research article ○ Abstract only

Microwave plasma oxidation kinetics of SiC based on fast oxygen exchange

Nannan You, Xinyu Liu, Jilong Hao, Yun Bai, Shengkai Wang

Article 109762

Purchase PDF Article preview

Research article ○ Abstract only

Optical testing method analysis of carrier transport in GaAs PCSS

Chongbiao Luan, Juan Zhao, Hongtao Li, Longfei Xiao, ... Yupeng Huang

Article 109771

Purchase PDF Article preview

Research article ○ Abstract only

Preparation and characterization of hierarchical nanostructures composed by CuO nanowires within directional microporous Cu

Yibo Ao, Jinqing Ao, Xiaoshan Yang, Ling Zhao, ... Xue Liu

Article 109774

Purchase PDF Article preview

Research article ○ Abstract only

Measurement of electron temperature and density of atmospheric plasma needle

S.S. Tabaie, D. Iraji, R. Amrollahi

Article 109761

Purchase PDF Article preview

Research article *Open access*

Reactive sputtering of CS_x thin solid films using CS_2 as precursor

Hans Högberg, Chung-Chuan Lai, Esteban Broitman, Ivan G. Ivanov, ... Gueorgui K. Gueorguiev

Article 109775

Download PDF Article preview

Research article ○ Abstract only

Combined experimental and DFT-TDDFT computational studies of doped $[PoDA+PpT/ZrO_2]^C$ nanofiber composites and its applications

Safwat A. Mahmoud, Ashjan A. Al-Dumiri, Ahmed F. Al-Hossainy

Article 109777

Purchase PDF Article preview

Research article ○ Abstract only

Parameter optimization of O_2/He atmospheric pressure plasma for surface modification of poly (L-lactic) acid oriented fiber membranes: Improving cell adhesion and proliferation

Shuneng Zhou, Li Wen, Zhenhua Tian, Karen Chang Yan, ... Gang Zou

Article 109763

Purchase PDF Article preview

Research article ○ Abstract only

Optical and electrical characterization of microwave power system chemical vapour deposited (MPS-CVD) graphene on Ni electroplated Cu foil at varying temperatures

John U. Arikpo, Michael U. Onuu

Article 109767

Purchase PDF Article preview

Research article ○ Abstract only

The effect of thickness on surface structure of rf sputtered TiO_2 thin films by XPS, SEM/EDS, AFM and SAM

Feyza Güzelçimen, Bükem Tanören, Çağlar Çetinkaya, Meltem Dönmez Kaya, ... Süleyman Özçelik

Article 109766

Purchase PDF Article preview

Research article ○ Abstract only

Synthesis, structural, optical and dispersion parameters of La-doped spinel zinc ferrites $ZnFe_{2-x}La_xO_4$ (x = 0.00, 0.001, 0.005, 0.01 and 0.015)

H. Lemziouka, A. Boutahar, R. Moubah, L.H. Omari, ... H. Lassri

Article 109780

Purchase PDF Article preview

Research article *Open access*

Comparisons of Theoretical and Experimental Results of Blue Light SiO_2–Nb_2O_5 Distributed Bragg Reflector Fabricated Using E-beam deposition

Zhan-Sheng Yuan, Jyum-Ming Jhang, Po-Hung Yu, Chiu-Man Jiang, ... Cheng-Fu Yang

Article 109782

Download PDF Article preview

Research article ○ Abstract only

Effect of TiC addition and Co binder content in cemented carbide substrates on the microstructure and mechanical properties of the TiAlN-based composite films

Lijun Xian, Haibo Zhao, Guang Xian, Ji Xiong, ... Hao Du

Article 109787

Purchase PDF Article preview

Research article ○ Abstract only

Self-lubricating and high wear resistance mechanism of silver matrix self-lubricating nanocomposite in high vacuum

Xiao Kang, Yang Sun, Lei Zhang

Previous vol/issue Next vol/issue

Vacuum 182 (2020) 109719

Contents lists available at ScienceDirect

Vacuum

journal homepage: http://www.elsevier.com/locate/vacuum

Improving the morphological, optical, and photocatalytic properties of octahedral Zn_2SnO_4 using *Garcinia mangostana* fruit peel extract

Eka Angasa [a,b], Yulia Eka Putri [a], Zulhadjri [a], Novesar Jamarun [a], Syukri Arief [a,*]

[a] *Materials Laboratory, Department of Chemistry, Andalas University, Padang, Indonesia*
[b] *Department of Chemistry, Bengkulu University, Bengkulu, Indonesia*

ARTICLE INFO

Keywords:
Octahedral Zn_2SnO_4
Garcinia mangostana
Fruit peel extract
Photodegradation

ABSTRACT

This study reports the successful synthesis of high purity Zn_2SnO_4 with octahedral microstructures through a green approach using *Garcinia mangostana* fruit peel extract. X-ray diffraction (XRD) patterns confirmed an enhanced crystallinity of the resulting sample. Meanwhile, morphology observation ascribed the formation of octahedral Zn_2SnO_4 by the using of 4% extract concentration. The results showed an increment in band gap energy from 3.26 eV to 3.38 eV. However, the synthesized Zn_2SnO_4 evidently favoured the improvement of photocatalytic performance for methylene blue (MB) degradation in terms of crystalline nature, grain size, and surface area expansion compared without the extract. These conclusions demonstrate the appropriate amount of extract applied possibly provides an effective additive in the control of crystallinity, morphology, and optical properties.

The unique properties of zinc tin oxide (Zn_2SnO_4), including wide band gap (3.6 eV), high electron mobility (10–15 $cm^2 V^{-1}s^{-1}$), superior electrical conductivity (~10^4 Scm^{-1}), attractive optical features, and low visible absorption confirm the known significance of the material [1–3]. Under these circumstances, the compound has been used in several widespread applications involving photocatalysts [4], gas sensors [5], DSSCs [2], and anodes for lithium-ion batteries [6].

Various synthetic techniques have been developed to improve Zn_2SnO_4 characteristics, including co-precipitation [7], solvothermal [8], hydrothermal [9], and sol gel [10]. In addition, separate mineralizers to increase crystallization, such as NH_4OH [10], NaOH [11], Na_2CO_3 [12], ethylamine, *n*-butylamine, *n*-hexylamine, and *n*-octylamine [13] have been employed. This prompts the necessity to control physicochemical and optoelectronic attributes for improved performance [14]. Therefore, two main influencing factors including morphology and size are achieved by applying additives. Previous reports indicated the use of hexadecyl trimethyl ammonium bromide (CTAB) (Ji, 2010) [11] and L-tryptophan (Li, 2012) [15] as capping/-stabilizing agents. Subsequently, both studies formed hexagonal nanoplate octahedral Zn_2SnO_4 with an edge size of 2–4 μm and 3 μm, respectively. However, excessive use of these chemicals appears disturbing due to ecological concerns. Hence, it is important to develop environmentally friendly methods for nanoparticle synthesis, e.g., green approach.

The green synthetic approach using plant extract has been rigorously extended to metal/metal oxide nanoparticle blends as a result of biomass and molecular abundance coupled with the ease of use [16–18]. In addition, primary compounds believed to be responsible for this blending process include amino acid, flavonoids, phenolics, heterocyclics, enzymes, tannins, saponins, polysaccharides, etc. [17]. Each compound shows the existence of separate active groups e.g. amino, –C–O–C–, –C–O–, –C═C–, and –C═O– [19,20], estimated to act collaboratively in metal ion reduction and surface stabilization [21,22]. For instance, phenolic compounds are believed as a substantial agent in metal/metal oxide synthesis. These compounds possess several active groups such as catechol, hydroxyl, and carbonyl which have capability in protonating and chelating or absorbing metal ion and reduce it into nanoparticle [17,23].

Various species and components of plants contain separate compounds targeted to determine the potential reduction and stabilizing/capping particles, hence the resulting metal/metal oxide shows dissimilar morphology, size, and activity [24]. Labanni et al. reported that silver nanoparticles prepared using *Uncaria gambir* leaf extract as reducing agent generated spherical shaped particles with size ranging between 6 and 39 nm [25]. However, silver nanoparticles prepared using *Garcinia mangostana* steam extract obtained agglomerated

* Corresponding author.
E-mail address: syukriarief@sci.unand.ac.id (S. Arief).

https://doi.org/10.1016/j.vacuum.2020.109719
Received 20 June 2020; Received in revised form 23 July 2020; Accepted 8 August 2020
Available online 26 August 2020

particles [26]. More analysis utilized *Garcinia mangostana* [27] and *Citrus aurantifolia* [28] fruit peel extracts both as reducing and capping agent to synthesize spherical and polyhedral shaped ZnO with average size of 21 nm and 9.7 ± 3 nm, respectively [27,28]. However, these representations are insufficient, especially in the synthesis of Zn–Sn–O material. The article on $ZnSnO_3$ synthesis using *Aspalathus linearis* produced quasi spherical shapes [29]. Subsequent synthesis outlined the use of glucose, sucrose, and starch as capping agent [30]. The application of three different-structured sugars resulted in Zn_2SnO_4 with different morphology and size. Furthermore, the nanoparticles prepared with glucose and sucrose were in the size range of 30–250 and 30–100 nm, respectively, but starch delivered nanoplates with thickness <100 nm.

This work is originally reported in an environmentally friendly process using plant extract in Zn_2SnO_4 synthesis. The paper further outlines an innovative approach by applying aqueous extract of *Garcinia mangostana* (mangosteen) fruit peel to obtain octahedral Zn_2SnO_4. Mangosteen peel contains highly phenolic compounds (xanthone) and a few other powerful biomolecules (flavonoids, benzophenones, and anthocyanin) that play important roles as capping/stabilizing agents for the synthesis of metal/oxide nanoparticles [26,27,31]. This work covers an attempt to prepare octahedral Zn_2SnO_4 with narrow size distribution and further investigated the effect of weight variation on crystallinity, morphology, and optical properties. Photodegradation ability towards MB was employed to evaluate photocatalytic performance.

These fruit peels were washed using tap and deionized water. The fruit peels were dried for 1 week, blended and then filtered using a Retsch test sieves (125 μm mesh size) to obtain a fine powder. Subsequently, aqueous extract was prepared by adding deionized water up to a total volume of 100 mL (2%, 4%, 6%, and 8% (w/v)) to the dust. The mixture was then stirred for 1 h and filtered using Hyunday paper No 10. Then, the entire extracts were stored in a refrigerator and prepared for Zn_2SnO_4 synthesis.

The samples were synthesized by the hydrothermal process. In addition, 10 mL of 0.1 M $Zn(CH_3COO)_2{\cdot}2H_2O$ (Merck, purity ≥99,5%) was mixed with 10 mL of 0.2 M $SnCl_4$ (Sigma Aldrich, purity 98%), and stirred at 800 rpm for 10 min. Then, 5 mL of aqueous extract was added and stirred for 10 min following the introduction of 20 mL of 0.4 M NaOH (Merck), and was left for 30 min (molar ratio of Zn^{+2}:Sn^{+4}:OH^- was 2:1:8). The final mixture volume of 45 mL was poured into a 100 mL Teflon lined stainless steel autoclave. This was heated at 185 °C for 18 h and left to cool at room temperature. The resulting sample was then filtered and washed repeatedly with deionized water. Finally, the product was dried at 85 °C for 16 h.

The crystallinity and phase of samples were studied by XRD (PAN analytical) with Cu Kα radiation at λ = 1.5406 Å. The morphology was scanned using scanning electron microscopy (SEM, FEI (Inspect-S50)) and transmission electron microscopy (TEM, JEM-1400). Subsequently, the optical absorption spectrum was characterized by UV–Vis Spectrophotometer (Analytik Jena, Specord 210), while surface area and pore size of prepared samples were calculated by the gas sorption analyzer using Quantachrome Instrument (Autosorb iQ Station 1) with BET and BJH methods.

The photocatalytic performance was measured by MB degradation in aqueous solution at room temperature. This experiment was conducted under three varying conditions, (i) without catalyst under UV light irradiation (blank) (ii) with catalyst in the absence of UV light irradiation (dark) (iii) with catalyst under UV light irradiation. Furthermore, 50 mg of synthesized Zn_2SnO_4 was added into 100 mL of 20 mg L^{-1} MB and stirred in dark for 30 min before irradiation to establish adsorption-desorption equilibrium. Then, the suspensions were exposed under a UV lamp (16 W, λ = 365 nm) where 3 mL of solution was withdrawn for every 15 min and centrifuged. Also, the absorption spectra were monitored using a T70 UV–Vis Spectrophotometer. These examinations were carried out in triplicate and all the data presented as mean ± standard deviation. Moreover, the significance of photodegradation efficiencies of Zn_2SnO_4 prepared with and without extract was determined by one-way ANOVA test by Analysis Toolpak program in Microsoft Excel.

X-ray diffraction patterns of Zn_2SnO_4 powder prepared in the presence and lack of extract corresponds to JCPDS standard (No. 01-074-2184). This was indexed to face centered-cubic spinel structured characterized by *Fd3m* space group of *Fd3m* (Fig. 1). The Zn_2SnO_4 prepared with extract showed a higher intensity and sharper peaks compared to samples without extract, indicating higher crystallinity, as shown in inset image of Fig. 1. In addition, the highest crystallinity was achieved by the sample prepared with the use of extract concentration at 4%, observed to decline as the extract quantity intensifies. The presence of impurities, including ZnO and SnO_2 were found in the sample prepared using 8% of extract. These results confirmed the mangosteen peel extract significantly influences the crystallinity and phase. The biomolecular functional groups such as the hydroxyl, have the ability to actively chelate Zn^{+2} and Sn^{+4} ions in well-defined sites, preventing agglomeration and crystal growth [22,32] in an effort to improve the crystallinity of the product. However, xanthones as major bioactive compounds are speculated to be more responsible for this situation.

Fig. 2 indicates the morphology of the synthesized Zn_2SnO_4 samples which were investigated by SEM and TEM. SEM images of the sample prepared using extract with concentration of 2% showed agglomerated particles in various forms (Fig. 2a). The particles with octahedral shape were discovered in the sample prepared using 4% of extract (Fig. 2b), while the samples using 6% of extract were slightly agglomerated spherical in shape (Fig. 2c). TEM images ensured the Zn_2SnO_4 particles were in an octahedral shape (Fig. 2d and e), as the formation of octahedral structure with edge length of 0.6–0.9 μm, was clearly observed to be similar with SEM. The hexagonal form was acquired by an electron beam focused on a triangle surface along the [001] zone axis of the octahedron (Fig. 2e) [14]. These results were compared with Zn_2SnO_4 prepared without extracts to further affirm the importance of applying extracts. However, the removal of the extract prompts the formulation of Zn_2SnO_4 with irregularly agglomerates, larger grain size, and no octahedron shaped particles (Fig. 2f). This shows the use of mangosteen peels with appropriate weight played a crucial role in octahedral formation. Therefore, the sample prepared using 4% extract was further analyzed by UV-DRS and the photocatalytic activity was examined through MB degradation.

Although the exact mechanism is still unknown, but literatures suggest that bioactive compounds contained in extract were responsible for the formation of octahedral Zn_2SnO_4. The active sites (hydroxyl, ketone, etc.) of biomolecules selectively bind with Zn (II) and Sn (IV) ions on the {1,1,1} termination surface, indicating a more positive surface {1,0,0} known to impede the reaction rate during the nucleation and particle development. This mechanism results in faster particle

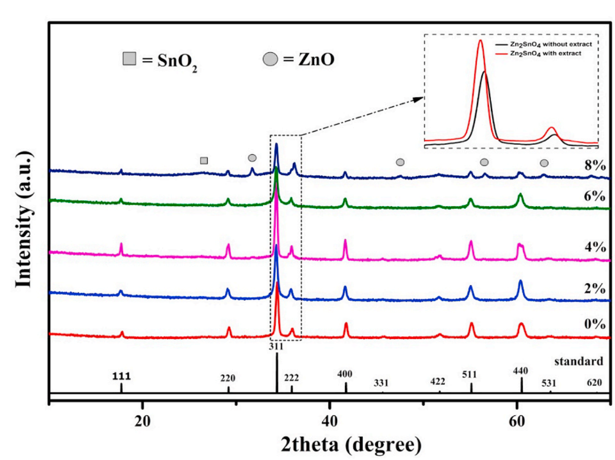

Fig. 1. XRD patterns of as-obtained Zn_2SnO_4 with various concentrations of extract.

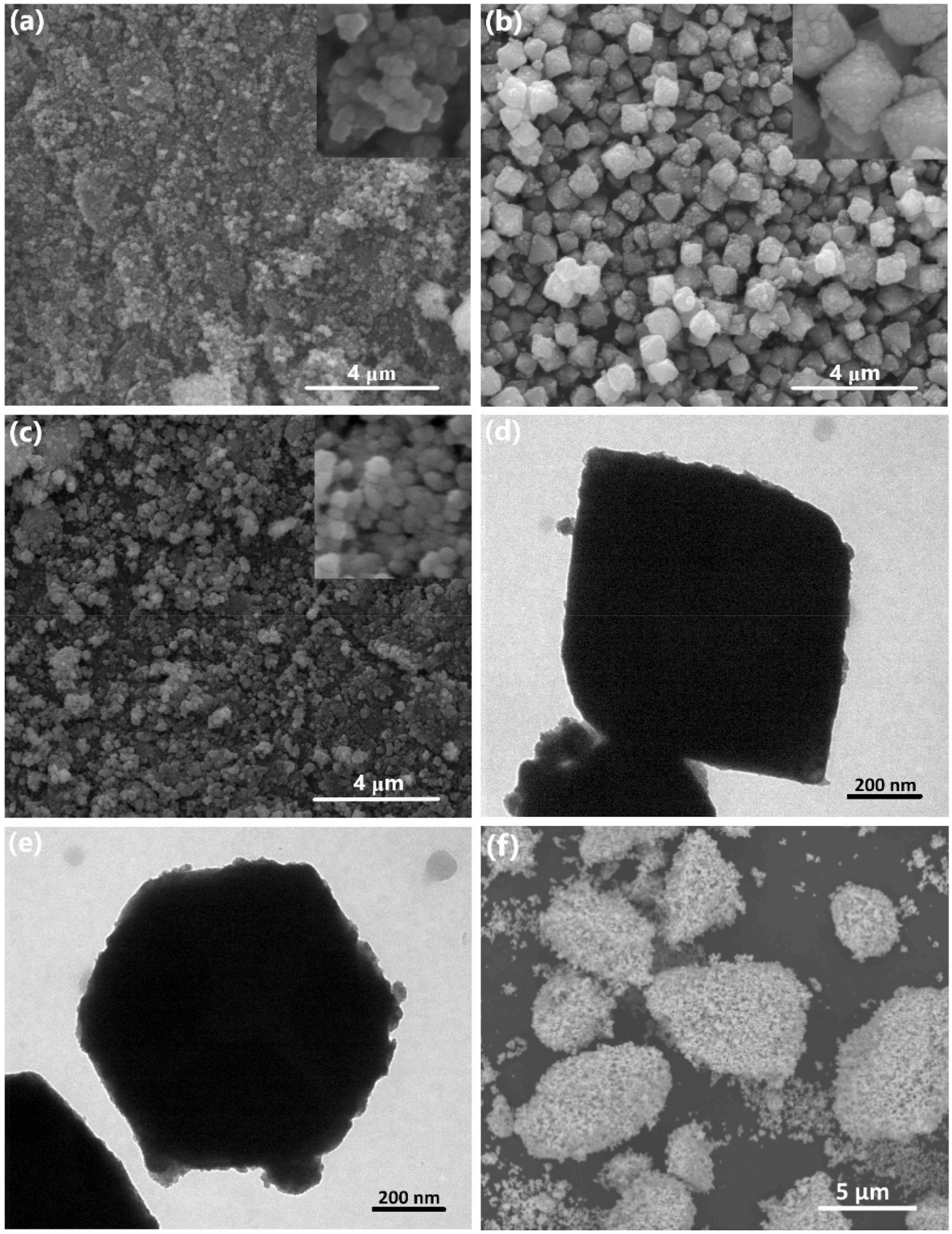

Fig. 2. (a–c) SEM images of Zn_2SnO_4 prepared using 2%, 4%, 6% of extract, respectively, (d,e) TEM images of octahedral Zn_2SnO_4, (f) SEM images of Zn_2SnO_4 prepared without extract.

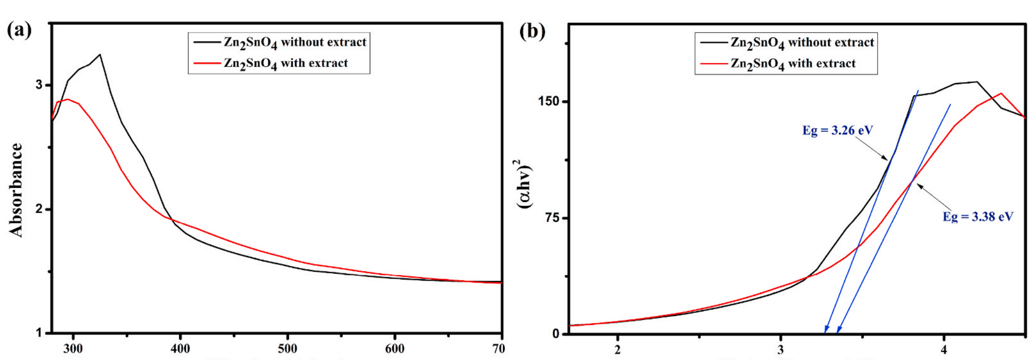

Fig. 3. (a) UV–Vis absorbance spectrum of as-synthesized Zn_2SnO_4, (b) Plot $(\alpha h\upsilon)^2$ vs hυ.

growth along {1,0,0} compared to {1,1,1}, hence generates Zn_2SnO_4 with octahedral structure [14]. In addition, the other bioactive compounds stabilize the particle surfaces resulting in octahedral Zn_2SnO_4 [21,22].

The UV–Vis DRS measurement of octahedral Zn_2SnO_4 exhibited a strong absorption spectrum slightly shorter in the range 300–400 nm compared without the extract (Fig. 3a). The steep curve of both samples indicated the light absorption originated from a band gap transition without interference from the impurity transition level. The optical band gap of octahedral Zn_2SnO_4 using Tauc's formula was known to increase by 3.38 eV compared to Zn_2SnO_4 prepared without extract, i.e. 3.26 eV (Fig. 3b). This increase is possibly due to changes in grain size initiated by improved morphology of octahedral Zn_2SnO_4 as shown in SEM images [30]. The band gap values of both samples were lower compared to the fundamental band gap of bulk Zn_2SnO_4 (3.60–3.70 eV). However, the resulted band gap of both samples ranged between several previous results, termed 3.2–3.9 [9,33,34]. Furthermore, the heat treatment applied tend to narrow the band gap to 3.25 due to the formation and incorporation of excess Zn in Zn_2SnO_4 matrix [35].

Fig. 4a shows the evolution of absorption spectra of MB solution during photodegradation by octahedral Zn_2SnO_4 under UV light at irradiation time interval. This observes the intensity of typical absorption peak of MB around 664 nm declined consecutively as the irradiation time increased. After 90 min, this peak highlighted low intensity due to the expiration of MB concentration. The rate of decrease in MB concentration at treatment time by using Zn_2SnO_4 octahedron was faster compared without the extract (Fig. 4b), indicating better photocatalytic performance. In addition, the photodegradation efficiencies of octahedral Zn_2SnO_4 and samples without extract after 90 min irradiation were $85.94 \pm 2.24\%$ and $78.93 \pm 2.87\%$, respectively. These results showed the photodegradation efficiency of octahedral Zn_2SnO_4 was significantly increased ($p < 0.05$), probably due to higher crystallinity of octahedral Zn2SnO_4 prepared using extract. The improvement of crystallinity leads to a decrease in probability of electron-hole recombination known to induce higher radical concentration and promote MB photodegradation. In addition, the morphology also plays a crucial role, where octahedral Zn_2SnO_4 with well aggregated and faceted particles observes higher specific surface area (Table 1). This provides more active surface sites in adsorbing the organic molecule, H_2O_2, OH^-, and O_2 [36,37] and these factors generated an increase in photodegradation efficiency and finally improve the photocatalytic activity. Fig. 4b also shows that the degradation rate of MB in absence of catalyst (blank) and dark condition was

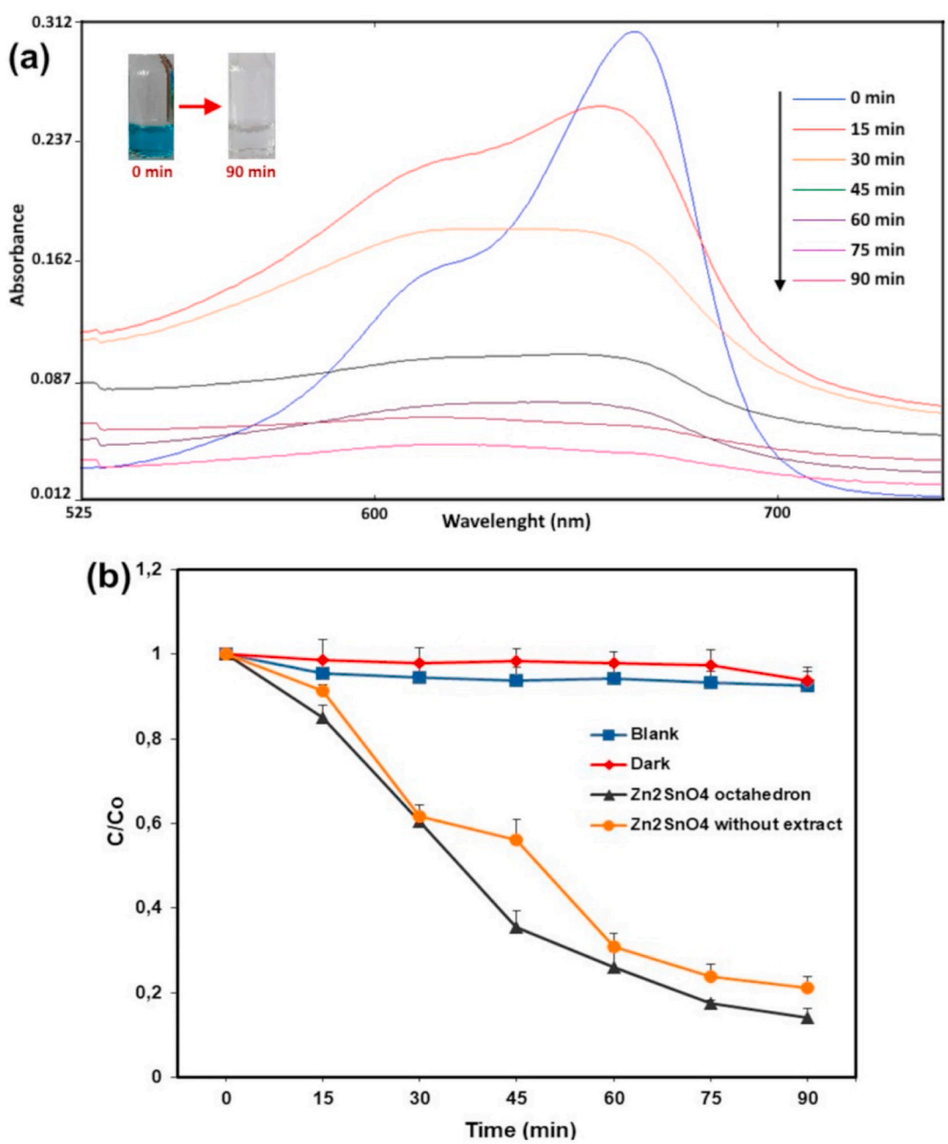

Fig. 4. (a) Degradation spectra of MB using Zn_2SnO_4 octahedron under irradiation of UV light (b) Degradation rate of MB with error bars of standard deviation as a function of irradiation time in different condition, in which C and Co are concentration of MB after and before treatment, respectively.

Table 1
The gas sorption analysis and degradation efficiencies of prepared Zn_2SnO_4.

No	Sample	Surface area (m^2/g)	Pore size (nm)	Pore Volume (cc/g)	Degradation Efficiency (%)
1	Zn_2SnO_4 prepared without extract	3452	1617	0,047	78.93 ± 2.87
2	Zn_2SnO_4 octahedron	5531	1616	0,060	85.94 ± 2.24

very slow and practically negligible. This result confirms the removal of MB was only caused by the degradation effect from prepared Zn_2SnO_4 under irradiation of UV light.

Conclusively, high purity Zn_2SnO_4 octahedron was synthesized through an environmentally friendly method by using *Garcinia mangostana* fruit peel extract. The use of extract with concentration of 4% instigates the formation of high crystallinity of the material with particles ranging from 0.6 to 0.9 μm. Meanwhile, the optical band gap of octahedral Zn_2SnO_4 was increased due to changes in grain size as a result of improved morphology. Based on analysis, the MB photodegradation efficiency using octahedral Zn_2SnO_4 was significantly higher compared to Zn_2SnO_4 without the extract due to crystallinity and morphology improvement and is significantly influenced by extract concentration. These results revealed the aqueous extract of *Garcinia mangostana* fruit peels as potential natural additives that further play an important role in Zn_2SnO_4 formation equipped with specific characteristics to enhanced the morphology, optical, and catalytic properties. Furthermore, the growth mechanism of octahedral Zn_2SnO_4 using *Garcinia mangostana* fruit peel extract deserves further investigation.

Declaration of competing interest

The authors declare that they have no known competing financial interests or personal relationships that could have appeared to influence the work reported in this paper.

Acknowledgments

This work was supported by the Lembaga Pengelola Dana Pendidikan (LPDP) of Ministry of Finance Indonesia under Grant No. PRJ-6090/LPDP.3/2016.

References

[1] L. Shi, Y. Dai, Synthesis and photocatalytic activity of Zn2SnO4 nanotube arrays, J. Mater. Chem. A. 1 (2013) 12981–12986, https://doi.org/10.1039/c3ta12388j.
[2] K. Al-Attafi, F.H. Jawdat, H. Qutaish, P. Hayes, A. Al-keisy, K. Shim, Y. Yamauchi, S.X. Dou, A. Nattestad, J.H. Kim, Cubic aggregates of Zn2SnO4 nanoparticles and their application in dye-sensitized solar cells, Nano Energy 57 (2019) 202–213, https://doi.org/10.1016/j.nanoen.2018.12.039.
[3] D. Hwang, J.S. Jin, H. Lee, H.J. Kim, H. Chung, D.Y. Kim, S.Y. Jang, D. Kim, Hierarchically structured Zn2SnO4 nanobeads for high-efficiency dye-sensitized solar cells, Sci. Rep. 4 (2014), https://doi.org/10.1038/srep07353.
[4] P.P. Das, P.S. Devi, D.A. Blom, T. Vogt, Y. Lee, High-pressure phase transitions of morphologically distinct Zn2SnO4 nanostructures, ACS Omega 4 (2019) 10539–10547, https://doi.org/10.1021/acsomega.9b01361.
[5] T.-T. Xu, Y.-M. Xu, X.-F. Zhang, Z.-P. Deng, L.-H. Huo, S. Gao, Enhanced H2S gas-sensing performance of Zn2SnO4 lamellar micro-spheres, Front. Chem. 6 (2018) 1–5, https://doi.org/10.3389/fchem.2018.00165.
[6] J. Xia, R. Tian, Y. Guo, Q. Du, W. Dong, R. Guo, X. Fu, L. Guan, H. Liu, Zn2SnO4-carbon cloth freestanding flexible anodes for high-performance lithium-ion batteries, Mater. Des. 156 (2018) 272–277, https://doi.org/10.1016/j.matdes.2018.06.056.
[7] D. An, Q. Wang, X. Tong, Q. Zhou, Z. Li, Y. Zou, X. Lian, Y. Li, Synthesis of Zn2SnO4 via a co-precipitation method and its gas-sensing property toward ethanol, Sensor. Actuator. B Chem. 213 (2015) 155–163, https://doi.org/10.1016/j.snb.2015.02.042.
[8] G. Sun, S. Zhang, Y. Li, Solvothermal synthesis of Zn2SnO4 nanocrystals and their photocatalytic properties, Int. J. Photoenergy 580615 (2014) 1–7, https://doi.org/10.1155/2014/580615.
[9] P.P. Das, A. Roy, S. Agarkar, P.S. Devi, Hydrothermally synthesized fluorescent Zn2SnO4 nanoparticles for dye sensitized solar cells, Dyes Pigments 154 (2018) 303–313, https://doi.org/10.1016/j.dyepig.2017.12.066.
[10] K.A. Bhabu, J. Theerthagiri, J. Madhavan, T. Balu, T.R. Rajasekaran, Synthesis and characterization of zinc stannate nanomaterials by sol-gel method, Mater. Sci. Forum 832 (2015) 144–157. https://doi.org/10.4028/www.scientific.net/MSF.832.144.
[11] X. Ji, X. Huang, J. Liu, J. Jiang, X. Li, R. Ding, Y. Hu, F. Wu, Q. Li, Hydrothermal synthesis of novel Zn2SnO4 octahedron microstructures assembled with hexagon nanoplates, J. Alloys Compd. 503 (2010) L21–L25, https://doi.org/10.1016/j.jallcom.2009.12.038.
[12] K. Kim, A. Annamalai, S.H. Park, T.H. Kwon, M.W. Pyeon, M.J. Lee, Preparation and electrochemical properties of surface-charge-modified Zn2SnO4 nanoparticles as anodes for lithium-ion batteries, Electrochim. Acta 76 (2012) 192–200, https://doi.org/10.1016/j.electacta.2012.04.121.
[13] X. Fu, X. Wang, J. Long, Z. Ding, T. Yan, G. Zhang, Z. Zhang, H. Lin, X. Fu, Hydrothermal synthesis, characterization, and photocatalytic properties of Zn2SnO4, J. Solid State Chem. 182 (2009) 517–524, https://doi.org/10.1016/j.jssc.2008.11.029.
[14] J. Nunez, F. Fresno, L. Collado, P. Jana, J.M. Coronado, D.P. Serrano, V.A. de la Pena O'Shea, Photocatalytic H2 production from aqueous methanol solutions using metal-co-catalysed Zn2SnO4 nanostructures, Appl. Catal. B Environ. 191 (2016) 106–115, https://doi.org/10.1016/j.apcatb.2016.03.020.
[15] Z. Li, Y. Zhou, J. Zhang, W. Tu, Q. Liu, T. Yu, Z. Zou, Hexagonal nanoplate-textured micro-octahedron Zn2SnO4: combined effects toward enhanced efficiencies of dye-sensitized solar cell and photoreduction of CO2 into hydrocarbon fuels, Cryst. Growth Des. 12 (2012) 1476–1481, https://doi.org/10.1021/cg201568q.
[16] M. Bandeira, M. Giovanela, M. Roesch-Ely, D.M. Devine, J. da S. Crespo, Green synthesis of zinc oxide nanoparticles: a review of the synthesis methodology and mechanism of formation, Sustain. Chem. Pharm. 15 (2020) 100223, https://doi.org/10.1016/j.scp.2020.100223.
[17] A.M. El Shafey, Green synthesis of metal and metal oxide nanoparticles from plant leaf extracts and their applications: a review, Green Process. Synth. 9 (2020) 304–339, https://doi.org/10.1515/gps-2020-0031.
[18] S. Matussin, M.H. Harunsani, A.L. Tan, M.M. Khan, Plant extract-mediated SnO2 nanoparticles: synthesis and applications, ACS Sustain. Chem. Eng. XXXX (2020), https://doi.org/10.1021/acssuschemeng.9b06398. XXX–XXX.
[19] J. Kesharwani, K.Y. Yoon, J. Hwang, M. Rai, Phytofabrication of silver nanoparticles by leaf extract of Datura metel: hypothetical mechanism involved in synthesis, J. Bionanoscience 3 (2009) 39–44, https://doi.org/10.1166/jbns.2009.1008.
[20] J. Huang, Q. Li, D. Sun, Y. Lu, Y. Su, X. Yang, H. Wang, Y. Wang, W. Shao, N. He, J. Hong, C. Chen, Biosynthesis of silver and gold nanoparticles by novel sundried Cinnamomum camphora leaf, Nanotechnology 18 (2007) 1–11, https://doi.org/10.1088/0957-4484/18/10/105104.
[21] S. Iravani, Green synthesis of metal nanoparticles using plants, Green Chem. 13 (2011) 2638, https://doi.org/10.1039/c1gc15386b.
[22] J. Jeevanandam, Y.S. Chan, M.K. Danquah, Biosynthesis of metal and metal oxide nanoparticles, ChemBioEng Rev 3 (2016) 55–67, https://doi.org/10.1002/cben.201500018.
[23] Q. Ye, F. Zhou, W. Liu, Bioinspired catecholic chemistry for surface modification, Chem. Soc. Rev. 40 (2011) 4244–4258, https://doi.org/10.1039/c1cs15026j.
[24] L.P. Silva, I.G. Reis, C.C. Bonatto, Green synthesis of metal nanoparticles by plants: current trends and challenges, in: Green Process, Nanotechnol., 2015, pp. 259–275, https://doi.org/10.1007/978-3-319-15461-9.
[25] A. Labanni, Zulhadjri, D. Handayani, S. Arief, Uncaria gambir Roxb. mediated green synthesis of silver nanoparticles using diethanolamine as capping agent, in: IOP Conf. Ser. Mater. Sci. Eng., 2018, https://doi.org/10.1088/1757-899X/299/1/012067, 299 012067.
[26] P. Karthiga, Preparation of silver nanoparticles by Garcinia mangostana stem extract and investigation of the antimicrobial properties, Biotechnol. Res. Innov. 2 (2017) 1–7, https://doi.org/10.1016/j.biori.2017.11.001.
[27] M. Aminuzzaman, L.P. Ying, W.-S. Goh, A. Watanabe, Green synthesis of zinc oxide nanoparticles using aqueous extract of Garcinia mangostana fruit pericarp and their photocatalytic activity, Bull. Mater. Sci. 41 (2018) 50, https://doi.org/10.1007/s12034-018-1568-4.
[28] O.J. Nava, C.A. Soto-Robles, C.M. Gomez-Gutierrez, A.R. Vilchis-Nestor, A. Castro-Beltran, A. Olivas, P.A. Luque, Fruit peel extract mediated green synthesis of zinc oxide nanoparticles, J. Mater. Sci. Mater. Electron. 1147 (2017) 1–6, https://doi.org/10.1016/j.molstruc.2017.06.078.
[29] N. Mayedwa, N. Mongwaketsi, S. Khamlich, K. Kaviyarasu, N. Matinise, M. Maaza, Green synthesis of Zin Tin Oxide (ZnSnO3) nanoparticles using Aspalathus linearis natural extracts: structural, morphological, optical and electrochemistry study, Appl. Surf. Sci. 446 (2018) 250–257, https://doi.org/10.1016/j.apsusc.2017.12.161.
[30] M. Masjedi-Arani, M. Salavati-Niasari, Effect of carbohydrate sugars as a capping agent on the size and morphology of pure Zn2SnO4 nanostructures and their optical properties, Mater. Lett. 174 (2016) 71–74, https://doi.org/10.1016/j.matlet.2016.03.084.
[31] J.S. Park, Y. Park, Asymmetric Dumbbell-Shaped Silver Nanoparticles and Spherical Gold Nanoparticles Green- Synthesized by Mangosteen (Garcinia Mangostana) Pericarp Waste Extracts, 2017, pp. 6895–6908.
[32] T. Khalafi, F. Buazar, K. Ghanemi, Phycosynthesis and enhanced photocatalytic activity of zinc oxide nanoparticles toward organosulfur pollutants, Sci. Rep. 9 (2019) 1–10, https://doi.org/10.1038/s41598-019-43368-3.

[33] M. Fakhrzad, A.H. Navidpour, M. Tahari, S. Abbasi, Synthesis of Zn2SnO4 nanoparticles used for photocatalytic purposes, Mater. Res. Express 6 (2019), https://doi.org/10.1088/2053-1591/ab2eb5.

[34] T. Jia, M. Liu, D. Yu, F. Long, S. Mo, Z. Deng, W. Wang, A facile approach for the synthesis of Zn2SnO4/BiOBr hybrid nanocomposites with improved Visible-light photocatalytic performance, Nanomaterials 8 (2018) 1–14, https://doi.org/10.3390/nano8050313.

[35] M.A. Alpuche-Aviles, Y. Wu, Photoelectrochemical study of the band structure of Zn2SnO4 prepared by the hydrothermal method, J. Am. Chem. Soc. 131 (2009) 3216–3224, https://doi.org/10.1021/ja806719x.

[36] A. Testino, I.R. Bellobono, V. Buscaglia, C. Canevali, M.D. Arienzo, S. Polizzi, R. Scotti, F. Morazzoni, Optimizing the photocatalytic properties of hydrothermal TiO2 by the control of phase composition and particle morphology. A systematic approach, J. Am. Chem. Soc. 129 (2007) 3564–3575, https://doi.org/10.1021/ja067050+.

[37] C.A. Emilio, M.I. Litter, M. Kunst, M. Bouchard, C. Colbeau-justin, Phenol photodegradation on platinized-TiO2 photocatalysts related to charge-carrier dynamics, Langmuir 22 (2006) 3606–3613, https://doi.org/10.1021/la051962s.